BROADBAND SCATTERING DATA INTERPOLATION BASED ON A RELAXED ADAPTIVE FEATURE EXTRACTION ALGORITHM

A. M. Raynal

Department of Electrical and Computer Engineering
The University of Texas at Austin
Austin, TX 78712, USA

J. T. Moore

SAIC
Champaign, IL 61820, USA

H. Ling

Department of Electrical and Computer Engineering
The University of Texas at Austin
Austin, TX 78712, USA

Abstract—A method using a relaxed adaptive feature extraction algorithm is investigated to interpolate broadband, high-frequency scattering from sparse, undersampled data. First, the adaptive feature extraction is extended to include a frequency-dependent scattering center model in order to better-describe broadband scattering physics from a complex target per the geometrical theory of diffraction. Second, the parameterization of the model is relaxed for more accurate extractions and a sparser model representation using fewer samples. Comparative results are presented for the relaxed versus the non-relaxed adaptive feature extraction algorithm for hypothetical examples and a numerically-solved ogive body of revolution. The relaxed algorithm is more computationally expensive, but results in significantly improved performance. The technique enhances adaptive feature extraction performance for broadband interpolation.

1. INTRODUCTION

The numerical solution of electromagnetic scattering from an electrically large and complex target over a broad frequency band can be a computationally expensive task. Using a frequency domain solver, the electromagnetic boundary value problem must be solved one frequency at a time. One means of decreasing the computation time and memory required to solve a problem is to use model-based parameter estimation (MBPE) [1–3]. This approach leverages a mathematical model that matches or approximates expected physical results in order to take fewer samples of an observable and interpolate unknown samples via the model. MBPE consists of two main components in practice: the model that approximates the problem physics and an algorithm for obtaining the model parameters. Once the model parameters are obtained from the available data, the interpolation (or extrapolation) can then be readily carried out using the model.

A commonly used model of high-frequency electromagnetic backscattering from complex targets is the scattering center model [4–8]. This model consists of a complex exponential series of frequency with complex amplitude coefficients. Based on the geometrical theory of diffraction (GTD), the amplitude coefficients are weakly frequency-dependent in the form of frequency raised to a power factor, which is well-known for certain canonical shapes only [6]. For broadband data interpolation or extrapolation, this frequency dependence is important. However, it is also challenging to parameterize accurately because the Cramér-Rao bound is extremely large compared to other model parameters [8]. Various schemes have been proposed on the extraction of the frequency dependence. Hurst and Mittra used a complex time-of-arrival model in conjunction with Prony's method to model the frequency dependence [4]. Moghaddar et al. applied a frequency pre-multiplier and a modified MUSIC algorithm in [5] to extract the frequency-dependent factor. Potter et al. utilized maximum likelihood algorithms for the same purpose [6]. Li et al. modeled broadband radar signatures through a genetic algorithm with adaptive feeding for both scattering and resonance behaviors [7]. The commonality amongst all these works is the use of an initial, dense data set over a broad frequency response in order to extract the sparse, scattering center model representation for use in radar feature extraction.

In contrast, Wang and Ling in [9] addressed the interpolation of broadband radar signatures from a sparsely, undersampled data set in order to save on data generation time using a computational electromagnetics solver. The model used is a scattering center model

for the currents on the target. The parameterization approach is based on an "adaptive feature extraction" (AFE) algorithm. Fundamentally, AFE can be considered a CLEAN [10] or matching pursuit [11] procedure whereby the model parameters are extracted one at a time using the maximum energy criterion. Random sampling in frequency is used intentionally to overcome the severe aliasing effects in the time domain that would otherwise occur for uniform sampling. However, higher sidelobes in time result from the sparse, random sampling and have a tendency to bury weak scatterers. The iterative extraction of scatterers in order of their energy contribution allows all scattering centers to be parameterized, including those adversely affected by the high sidelobe interference. The results of [9] demonstrated a significant reduction in the number of frequency samples needed to represent electromagnetic scattering data when compared to the Nyquist sampling under uniform sampling. However, a scattering center model without any frequency dependence was used in the work, which does not parameterize broadband data adequately. Further, since the model was applied to the currents, an interpolation was needed for each current element on a target, leading to somewhat large computational demands.

In this paper, we improve upon the work in [9] by utilizing the frequency-dependent scattering center model for the interpolation of sparsely-sampled, broadband radar signature data. We compare two parameterization approaches. In the first approach, we simply extend the AFE procedure to estimate the frequency-dependence parameter in addition to the arrival time and scattering center amplitude. In the second approach, we adapt the RELAX algorithm proposed by Li and Stoica [12] to improve upon the estimation of the model parameters. RELAX was originally devised in order to relieve error propagation tendencies in the CLEAN algorithm for the frequency-independent scattering center model and has been applied to dense, uniformly sampled data. The motivation for using RELAX is that it redistributes the energy of identified scatterers, or relaxes their parameter values, iteratively, to obtain more accurate feature extraction. In our problem, relaxation is especially important since the frequency-dependence factor is difficult to estimate accurately. To the best of our knowledge, the use of RELAX on the frequency-dependent scattering center model and a sparse, randomly sampled data set has not been reported in the past.

This paper is organized as follows. Section 2 progressively elaborates on the modified AFE algorithm with frequency-dependent scattering center model and then the relaxed AFE algorithm. Section 3 contains a comparison of results for hypothetical examples and

computational electromagnetics data for an ogive body of revolution with the relaxed and non-relaxed algorithms. Finally, a concluding summary is provided in Section 4.

2. EVOLUTION OF THE RELAXED AFE FREQUENCY-DEPENDENT MODEL ALGORITHM AND METHODOLOGIES

2.1. The Frequency-Dependent Model

The model for the backscattered electric field, E, of multiple time-of-arrival events from ray-optical behaviors can be written as an exponential function of frequency [4–8]:

$$E(f) = \sum_n a_n \left(\frac{f}{f_c} \right)^{\alpha_n} e^{-j2\pi f t_n} = \sum_n a_n \varphi_n, \qquad (1)$$

where a_n is an amplitude coefficient, and α_n is a real-valued exponent to account for the frequency-dependent amplitude. The center frequency, f_c is included for normalization. Equation (1) models the scattered field at high frequencies as a sum of discrete time events, each with a time of arrival, t_n. The equation can also be thought of as a synthesizing map of the set of amplitude coefficients of scattering centers with a basis function, φ_n, that includes the time of arrival, t_n, and frequency-dependence parameter of the corresponding scattering centers.

2.2. The AFE Algorithm for the Frequency-Dependent Model

Next, an algorithm is sought to find the model parameters in (1) by using an undersampled set of data points of $E(f)$. One way to accomplish this parameterization efficiently is the AFE algorithm, which was developed for a frequency-independent model [9]. A key concept of AFE is to use randomly sampled points of $E(f)$ in order to overcome the Nyquist sampling requirement. The algorithm then iteratively searches for the basis function that extracts the maximum energy out of the signal. After each iteration, the contribution of the best matched basis is removed from the original signal to reveal weaker scatterers. Here we extend the original AFE algorithm to the frequency-dependent model as follows:

1. Given N random data samples from $E(f)$ at known frequencies, f_k, compute the analyzing mapping for a discrete set of time samples, t_i,

and a range of amplitude frequency-dependent exponents, α_i:

$$a_i = \frac{\langle E(f), \varphi_i \rangle}{\langle \varphi_i, \varphi_i \rangle} = \frac{\sum_{k=1}^{N} E(f_k) \left(\frac{f_k}{f_c}\right)^{\alpha_i} e^{+j2\pi f_k t_i}}{\sum_{k=1}^{N} \left(\frac{f_k}{f_c}\right)^{2\alpha_i}}. \qquad (2)$$

2. Compute the energy of every potential solution for the synthesizing map, that is, the inner product of every $a_i \varphi_i$ with itself, which yields:

$$\langle a_i \varphi_i, a_i \varphi_i \rangle \|a_i \varphi_i\|^2 = |a_i|^2 \frac{1}{N} \sum_{k=1}^{N} \left(\frac{f_k}{f_c}\right)^{2\alpha_i}. \qquad (3)$$

3. Select the time and frequency exponent pair $\{t_n, \alpha_n\}$ that result in the maximum energy basis (i.e., $\max\{\|a_i \varphi_i\|^2\}$) and find the corresponding amplitude coefficient, a_n from step 1. The set $\{a_1, \alpha_1, t_1\}$ represents the strongest scatterer in the data.
4. Synthesize the strongest scatterer and subtract it from the known $E(f)$ to compute a residual, $R(f)$, where $R_1(f) = E(f) - a_1 \varphi_1$.
5. By removing the strongest scatterer from the signal in frequency, the second strongest scatterer becomes more apparent when the analyzing mapping is carried out on the residual, $R(f)$, since the stronger scatterer is no longer contributing energy. Therefore, steps 1–4 are repeated to find the second strongest scatterer and a new residual, $R_i(f) = R_{i-1}(f) - a_i \varphi_i$ can be computed. This process is iterated until finally all the scatterers have been identified and the residual is at the noise floor level.

Once AFE is complete, a synthesis mapping using all scattering centers $\{a_n, \alpha_n, t_n\}$ and a large frequency set in the bandwidth of interest can reproduce a dense $E(f)$ solution. Two comments are in order for the algorithm implementation. First, based on the geometrical theory of diffraction, the range in α_i is limited for canonical shapes. For instance, corner diffraction is of order f^{-1}; edge diffraction is of order $f^{-1/2}$; doubly curved surface reflections such as from spheres, and straight edge specular diffraction are of order f^0; singly curved surface reflections such as from cylinders are of order $f^{1/2}$, broadside flat plates or dihedral reflections are of order f^1 [6, 8]. In our implementation, we restrict our search to the range $[-2, 2]$ in half integer steps.

Second, to save computation time on the search for t_n and obtain accurate results, a tree search is implemented. We use a somewhat coarse t_i to find a preliminary maximum amplitude coefficient and

corresponding time, i.e., $\{a_n, \alpha_n, t_n\}$. Then the search space in time is focused in a window about the found preliminary values by a finer set of t_i. AFE is then restarted with the new search space, and a new maximum a_n, α_n and refined t_n are found. This zoom-in process continues until the value of t_n stabilizes between levels of the tree search, at which point $\{a_n, t_n\}$ is defined for that AFE iteration and the remaining steps of AFE are carried out. Such a tree search for the frequency-dependence dimension is unnecessary because the energy characteristics across the range in α_n are subtle as compared to the dramatic properties exhibited for a discrete-time event.

2.3. The Relaxed AFE Algorithm for the Frequency-Dependent Model

The AFE procedure is based on the premise that the extraction of the strongest scattering center is not biased in any way by the weaker scatterers. This situation is not exactly true, especially when there is strong mutual interference among the bases. The result is error propagation in the AFE algorithm. A solution to overcome this problem is the RELAX procedure proposed in [12]. Here, we extend the procedure to deal with the frequency-dependent model. The relaxation algorithm serves the purpose of redistributing the energy of each scatterer extracted in every AFE iteration by adjusting and readjusting the found values of $\{a_n, \alpha_n, t_n\}$ of all extracted scatterers leading up to the current AFE iteration in an inner iterative loop. Consequently, the mutual interference effects that cause inaccurate scatterer extractions are "relaxed" and hopefully improved by this readjustment of the initially found parameter values.

Relaxation occurs in the AFE algorithm once the second strongest scatterer has been found. At that stage, the second scatterer's contribution is extracted from the original signal. The goal is to more accurately extract the first and strongest scatterer a second time, without the mutual interference effects of the second scatterer. The re-extraction of the two scatterers repeats until convergence. Afterwards, the AFE algorithm resumes in order to extract the next strongest scatterer from the residual. The relaxation process is then initiated again to individually adjust the values of all known scatterers in the absence of the contribution of the others. More formally, the RELAX process that is integrated into each AFE iteration is defined as follows.

1-3R. Compute steps 1–3 of the AFE algorithm.
Given an AFE iteration $i > 1$:
4R. Find the AFE iteration residual, $R_i(f_k) = E(f_k) - \sum_{n=1}^{i} a_n^x \varphi_n^x$, where x denotes the final jth adjustment by RELAX to the parameter

values of all scatterers in the prior AFE iteration or in other words the most current parameter values known for each scatterer.

5R. Use the AFE iteration residual to compute steps 1-3R to find the initial $\{a_n, \alpha_n, t_n\}^{j=0}|_{n=i+1}$ of the next strongest scatterer in the data.

6R.

   a. Begin RELAX by letting $j = 1$.

   b. Let $n = 1$.

   c. Synthesize all scatterers $m \neq n$ and subtract them from the known $E(f_k)$ to compute a RELAX iteration residual, $R_m^j(f_k)$, where $R_m^j(f_k) = E(f_k) - \sum_{m=1}^{i} a_m^{j-1} \varphi_m^{j-1}$.

   d. Repeat steps 1-3R on the RELAX residual $R_m^j(f_k)$ to find new adjusted values for the scatterer $\{a_n, \alpha_n, t_n\}^j$.

   e. Increase n by one and repeat steps 6Rc-e for all n up to and including $n = i$.

   f. If the relative change between the parameters $\{a_n, \alpha_n, t_n\}^{j-1}$ and $\{a_n, \alpha_n, t_n\}^j$ has not reached convergence and/or j does not equal a maximum iterative value, increase j by one and repeat steps 6Rb-f.

RELAX is completed for each AFE iteration, except the first. Once AFE with RELAX is complete, a synthesis mapping using all finalized, relaxed scattering centers $\{a_n, \alpha_n, t_n\}$ and a large frequency set in the bandwidth of interest can reproduce a dense $E(f)$ solution. Note that the cost function chosen in step 6Rf varies from the suggested computation of relative rms error in the RELAX paper of Li and Stoica [12]. This modification is done in the interest of computation time.

3. RESULTS OF RELAXED AND NON-RELAXED AFE WITH FREQUENCY-DEPENDENT MODEL

3.1. Point-Scatterer Examples

The AFE algorithm with the frequency-dependent model was applied with and without parameter relaxation to hypothetical examples whereby truth frequency data of 1000 points was generated via the synthesizing map for a few point-scatterers. The motivation for these examples is to obtain a general idea of the performance of the algorithms for small and large bandwidths and different positionings of the point-scatterers relative to the bandwidth. The rms error stopping criteria for the algorithms was set to 1% error ($-40\,\text{dB}$). The results presented in this and the next section observe the following format: Figure 1(a) demonstrates rms error performance in decibels

compared to the truth data for AFE (asterisked-solid line) and relaxed
AFE (x-dashed line), as a function of the number of data samples
taken, N; Figure 1(b) shows $|a_n|$ in decibels as a function of time in
nanoseconds for AFE (asterisk), relaxed AFE (circle), and the truth
(x in hypothetical examples) data; and Figure 1(c) shows $|E(f)|$ in
decibels as a function of frequency in gigahertz for AFE (long dash,
short dashed line), relaxed AFE (short dashed line), and the truth
(solid line) data.

The first example consists of three scatterers with $a_n =$
$\{5, 10, 1\}$, $\alpha_n = \{1.5, 2, -1\}$, $t_n = \{25\,\text{ns}, 50\,\text{ns}, 75\,\text{ns}\}$ with desired
results shown in Figure 1 over a $2\,\text{GHz}$ bandwidth from 9–$11\,\text{GHz}$.
Given the overall time extent of the scatterers of $50\,\text{ns}$, the Nyquist
criterion is expected to be $N = 100$ data samples (i.e., $50\,\text{ns}*2\,\text{GHz}$).
As seen in Figure 1(a), both AFE and relaxed AFE are well under the
Nyquist criterion in terms of the number of data samples required to
get within 1% rms error of the truth data. However, AFE achieves only
about 3.2 times the savings at $N = 31$, whereas relaxed AFE achieves
14.2 times the savings with $N = 7$. The rms error that reaches the
stopping criteria is also lower for relaxed AFE than AFE (0.52% versus
0.94%). Note that the rms error is not monotonically decreasing for
AFE. In general, this result is not uncommon for either algorithm (as
will be seen in the next example for relaxed AFE). The phenomenon is
due to the randomly chosen data samples which may or may not add
useful information to the algorithm as additional samples are taken.
In Figure b), the number of iterations, i, which translates into the
number of scatterers estimated by the algorithms can be observed to
be much closer to the truth value of three for relaxed AFE ($i = 5$),
than AFE ($i = 20$). The time data further illustrates how relaxed AFE
tends to be more accurate in ascertaining the correct parameters of the
scatterers than AFE by comparison of the location of all tick marks.
Figure 1(c) shows that both algorithms achieve a good synthesized
solution in frequency that is hardly distinguishable from the truth data,
despite the approximations made.

The case depicted in Figure 2 is again three point-scatterers with
similar center frequency of $10\,\text{GHz}$, a_n, and α_n as compared to the
first example but with $t_n = \{-2.5\,\text{ns}, 0\,\text{ns}, 2.5\,\text{ns}\}$ over a $16\,\text{GHz}$-wide
band from 2–$18\,\text{GHz}$. For such broadband data, we have found that
the use of the frequency-independent model was not able to yield an
accurate parameterization for a reasonable number of data samples.
The Nyquist sampling is given by $N = 80$ ($5\,\text{ns}*16\,\text{GHz}$). AFE reaches
0.98% rms error as compared to the truth with $N = 34$, indicating
about 2.4 times the savings to Nyquist, and the number of scatterers
remains unchanged from before. Relaxed AFE reaches 0.018% rms
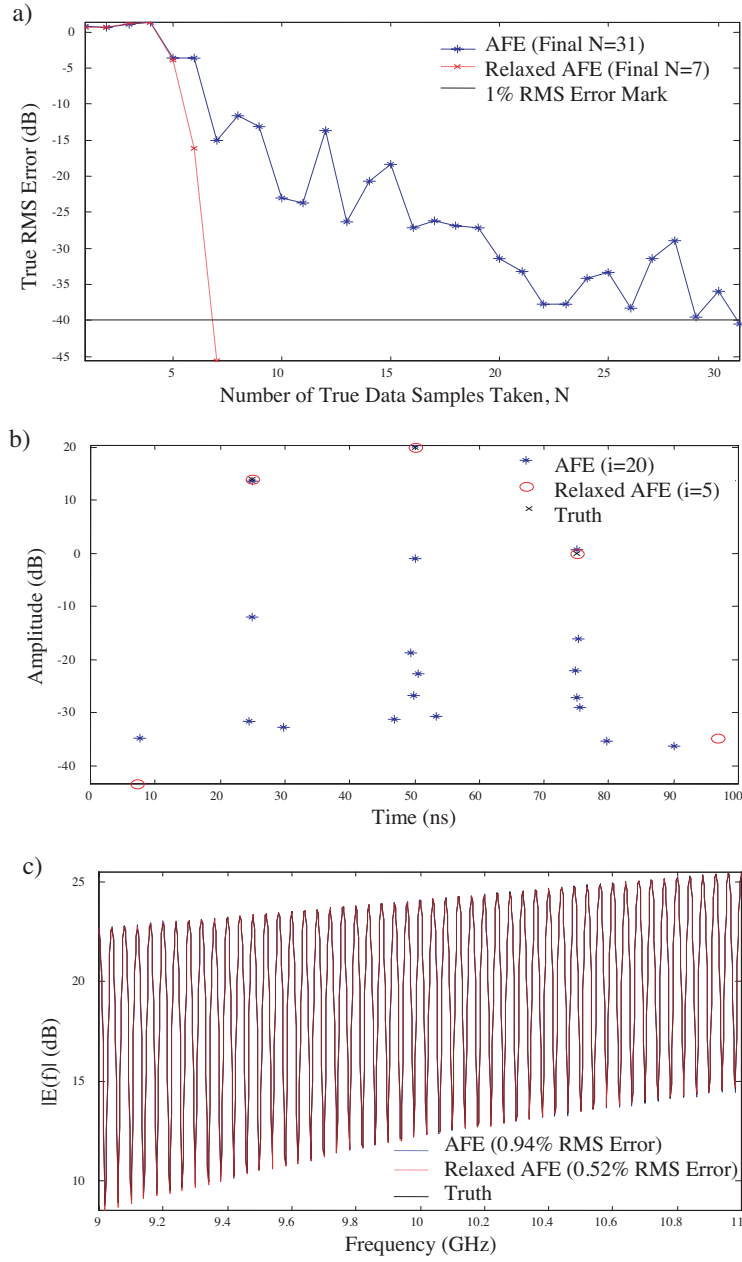
a)

b)

c)

Figure 1. Three far apart scatterers, 2 GHz bandwidth high-frequency data with parameters $a_n = [5, 10, 1]$, $t_n = [25, 50, 75]$ ns, and $\alpha_n = [1.5, 2, -1]$.

error as compared to the truth, which is much lower than AFE by about
34.7 dB as shown in Figure 2(a). Relaxed AFE also has $N = 15$ for
about 5.3 times savings versus the Nyquist criterion and $i = 8$, which
is still much lower than AFE. The lack of monotonicity in rms error
for both algorithms can be noted in Figure 2(a) as well. Figure 2(b)
shows more extraneous scatterers for the relaxed AFE as compared
to Fig. 1(b) due to the larger bandwidth. However, the agreement
between the synthesized frequency data and the reference for both
algorithms is still quite satisfactory, as shown in Figure 2(c).

The last hypothetical example seeks to explore a worst case for
the algorithms. The prior three-scatterer wideband case is adopted
with an additional, weak scatterer with parameters $\{a_n, \alpha_n, t_n\} =$
$\{1, -0.5, -0.125 \, \text{ns}\}$. Figures 3(a)–(c) recap similar trends as in the
prior example, that is, lower N, i, and rms error for relaxed AFE versus
AFE and a greater savings in N as compared to Nyquist with a more
accurate parameter estimation. The positioning of the fourth scatterer
very close to the one at 0 ns along with the other far away scatterers has
the effect of gradually modulating the envelope of the frequency data
in Figure 3(c) versus Figure 2(c). This data set is more challenging to
estimate because close scatterers' sidelobe structures will interfere to a
greater extent, masking the parameters of the scatterers more severely.
In effect, AFE performance degrades to $N = 42$, $i = 25$, and 0.91%
rms error, indicating a mere 1.9 times savings versus Nyquist. Relaxed
AFE also struggles more. Nevertheless, it yields $N = 19$, $i = 10$, and
0.031% rms error, for a 4.2 times savings as compared to the Nyquist
criterion.

To summarize, in all the test cases, relaxed AFE outperforms AFE
alone. In particular, AFE is highly susceptible to error when selecting
the frequency-dependence factor, α_n, since the distinction in energy
versus alpha-space is very slight. Given that the relaxation algorithm
is made for such mutual interference, it is able to fine-tune the α_n
selection for each scatterer more accurately.

3.2. 3D-Ogive Results

Having developed an understanding of the performance trends of the
two algorithms with hypothetical examples, the revised AFE algorithm
with the frequency-dependent model was applied with and without
parameter relaxation to an ogive body of revolution 0.3 m long and
0.06 m across at its widest point as depicted in Figure 4. The frequency
range for the scattered electric field was 3 to 15 GHz. The Nyquist limit
for the object is thought to be roughly 60 points since the bandwidth is
12 GHz and the time extent of scatterers is near 5 ns depending on the
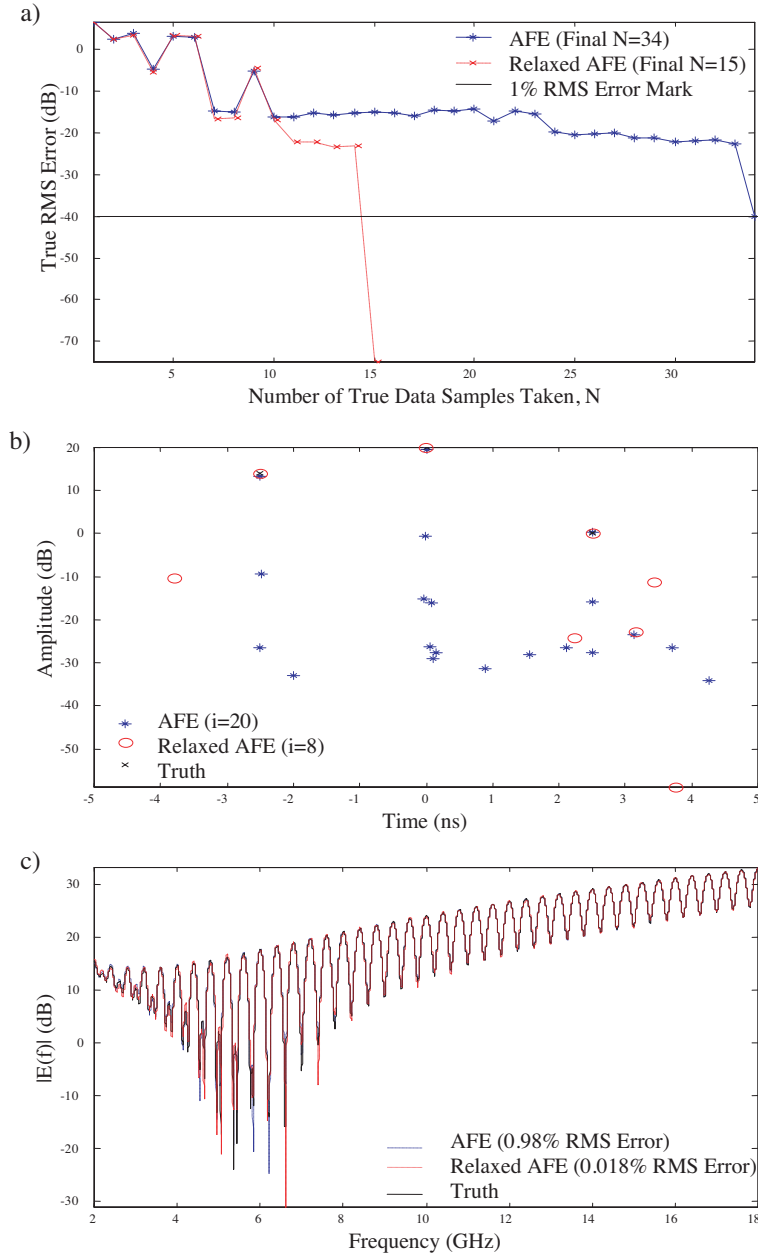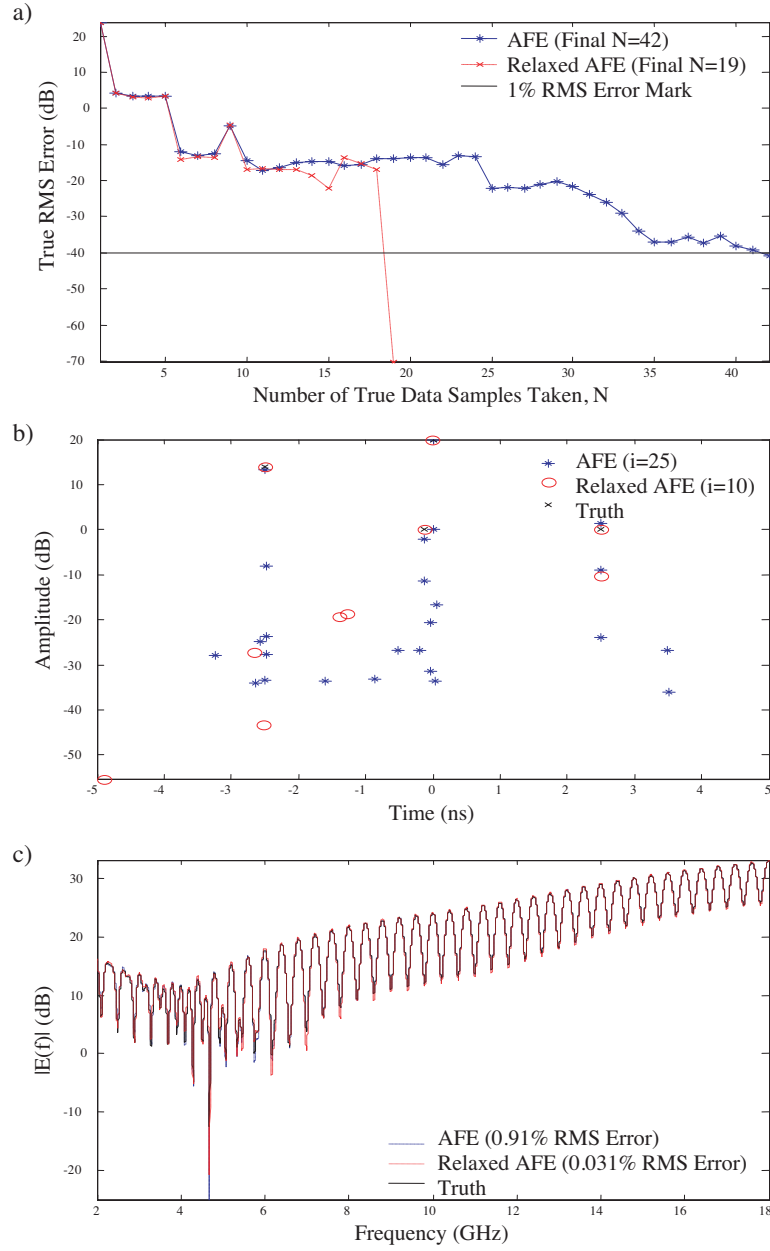angle of incidence. A body-of-revolution method of moments solver

Figure 2. Three far apart scatterers, $16\,\mathrm{GHz}$ bandwidth high-frequency data with parameters $a_n = [5, 10, 1]$, $t_n = [-2.5, 0, 2.5]\,\mathrm{ns}$, and $\alpha_n = [1.5, 2, -1]$.

Figure 3. Four close and far apart scatterers, $16\,\mathrm{GHz}$ bandwidth high-frequency data with parameters $a_n = [5, 10, 1, 1]$, $t_n = [-2.5, 0, -0.125, 2.5]\,\mathrm{ns}$, and $\alpha_n = [1.5, 2, -0.5, -1]$.
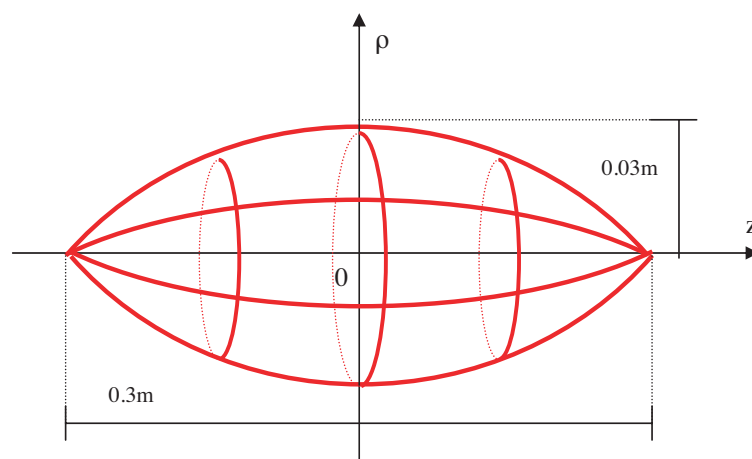
Figure 4. Ogive body of revolution.

was used to generate 121 data sample points for reference. The extent of the initial time window for the algorithm search, t_i, was from $-5\,$ns to $+5\,$ns. Lastly, the incident electric field was polarized in theta.

Figure 5 shows the algorithm results for an incident angle theta=60°. This angle data resembles the second hypothetical example of Figure 2 in that it depicts a wideband case, where the scatterers appear to be somewhat far apart. AFE performs terribly with $N = 100$, which is not below Nyquist, $i = 14$, and only achieving a 10% rms error as compared to the truth data. Relaxed AFE shows some promise, with N=27 which is 2.2 times better than the Nyquist criterion, $i = 8$, and achieving a 7.8% rms error. Once again, relaxed AFE performs better than AFE and Nyquist, though for a higher rms error criteria. Upon observation of Figure 5(c), one notices that the synthesized frequency data seems to be in close agreement with the truth data for relaxed AFE, where the two curves are nearly indistinguishable. AFE on the other hand, clearly does not agree as well throughout, especially in the frequency regions from 12 to 14 GHz.

Figure 6 shows results at theta=30°. This angle data resembles the last hypothetical example, where a wideband case with scatterers positioned in mixed, close and far proximity was discussed to cause gradual modulation of an envelope of faster-modulated frequency data in Figure 3(c) and Figure 6(c) and increased mutual interference. In fact, in Figure 6(b) the scatterers are so close in time that they are not resolved by the IFFT, but rather lumped together as a very wide scatterer. As expected, AFE performance is poor with $N = 97$, $i = 25$,
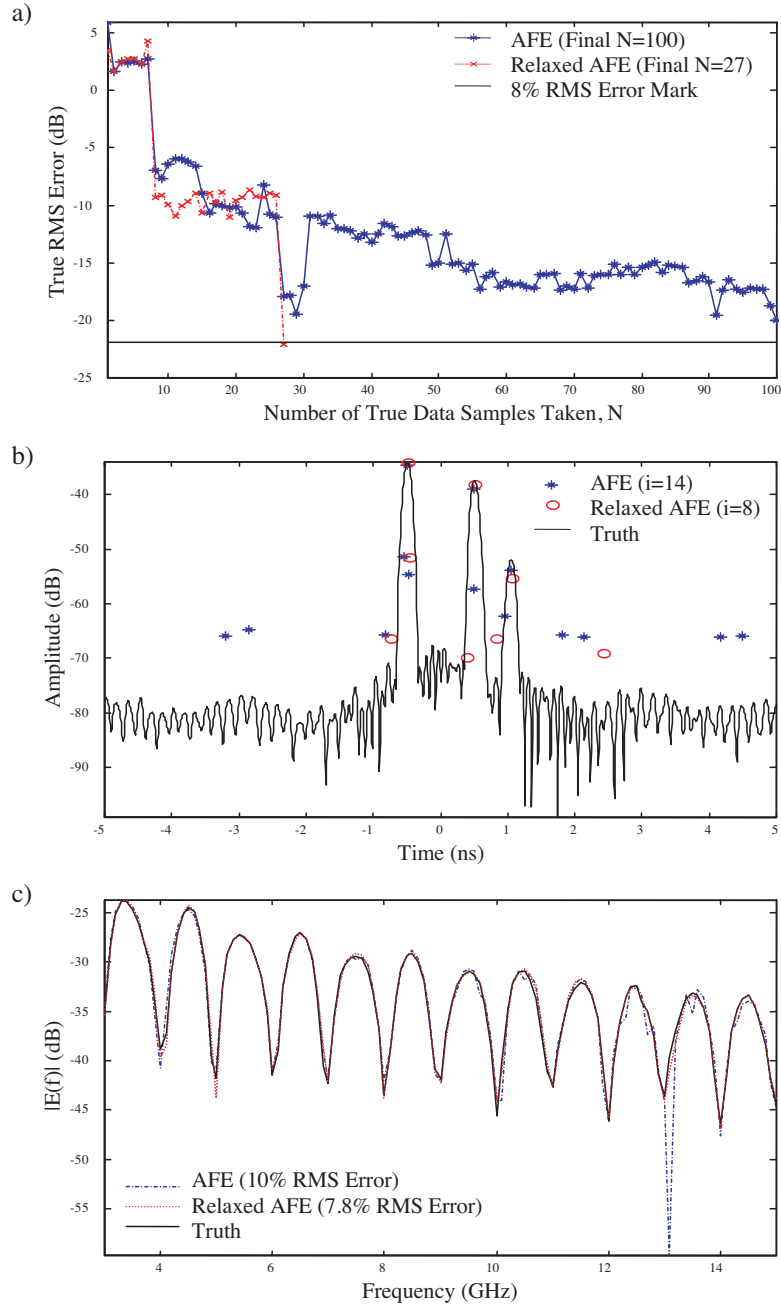
a)

b)

c)

Figure 5. Ogive theta=60°, 12 GHz bandwidth high frequency data.

a)

b)

c)

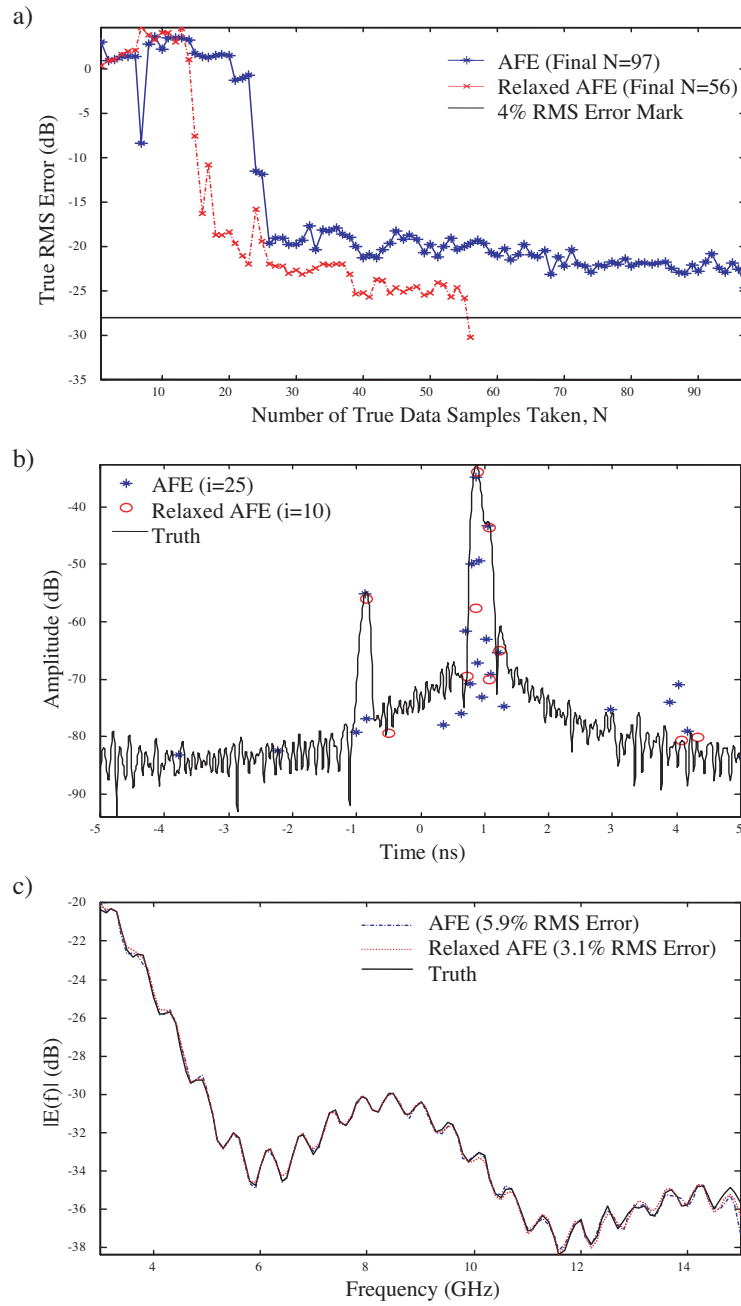**Figure 6.** Ogive theta=30°, 12 GHz bandwidth high frequency data.

and 5.9% rms error. Relaxed AFE results show $N = 56$, $i = 10$, and 3.1% rms error. Though relaxed AFE did not perform as well for the ogive as for the hypothetical example, it still clearly surpassed AFE's performance. The rms error and the agreement of the synthesized frequency solution are again satisfactory.

We should point out that the ogive is an extremely challenging target for interpolation at certain angles because of its creeping wave physics. For example, the girth of the second peak near 1 ns in Figure 6(b) and disturbances in the surrounding sidelobe structures of the IFFT are clear indication that the peak is actually an amalgamation of at least 4 or 5 unresolved discrete-time events. Closer examination of the travel times from the many possible creeping wave mechanisms confirms this observation. Therefore, the larger number of points required for successful interpolation is not surprising, even with the relaxed AFE algorithm.

4. SUMMARY

In conclusion, the broadband interpolation of electromagnetic backscattering data from a sparsely computed data set in frequency has been investigated. The previously developed AFE algorithm has been improved to include a frequency-dependent model and parameter relaxation. The revised model accommodates a well-known frequency dependence in the amplitude term of the exponential series. This model more accurately describes high-frequency time-of-arrival physics in accordance with ray-optics. AFE uses random sampling and matching pursuit to eliminate aliasing and allow for fewer electromagnetic solver data points than those dictated by the Nyquist criterion for equal sampling algorithms. Further, we have implemented a parameter relaxation version of AFE to reduce the error in selecting the frequency dependence of the scattering centers, which have subtle energy characteristics. The improved extraction is accomplished by redistributing the energy of scatterers found by the algorithm through an iteration process. Comparative results have been presented for the relaxed versus the non-relaxed adaptive feature extraction algorithm for hypothetical examples and a numerically-solved ogive body of revolution. The relaxed algorithm is more computationally expensive, but results in significantly improved performance. The technique enhances adaptive feature extraction performance for broadband signature interpolation.

REFERENCES

1. Miller, E. K., "Model-based parameter estimation in electromagnetics: Part I. Background and theoretical development," *IEEE Antennas and Propagation Magazine*, Vol. 40, No. 1, 42–52, Feb. 1998.

2. Miller, E. K., "Model-based parameter estimation in electromagnetics: Part II. Applications to EM observables," *IEEE Antennas and Propagation Magazine*, Vol. 40, No. 2, 51–65, Apr. 1998.

3. Miller, E. K., "Model-based parameter estimation in electromagnetics: Part III. Applications to EM integral equations," *IEEE Antennas and Propagation Magazine*, Vol. 40, No. 3, 49–66, June 1998.

4. Hurst, M. P. and R. Mittra, "Scattering center analysis via Prony's method," *IEEE Trans. Antennas Propagat.*, Vol. 35, 986–988, Aug. 1987.

5. Moghaddar, A., Y. Ogawa, and E. K. Walton, "Estimating the time-delay and frequency decay parameter of scattering components using a modified MUSIC algorithm," *IEEE Transactions on Antennas and Propagation*, Vol. 42, No. 10, 1412–1418, Oct. 1994.

6. Potter, L. C., D. M. Chiang, R. Carriere, and M. J. Gerry, "A GTD-based parametric model for radar scattering," *IEEE Transactions on Antennas and Propagation*, Vol. 43, 1058–1067, Oct. 1995.

7. Li, J., Y. Zhou, and H. Ling, "Sparse parameterisation of electromagnetic scattering data using genetic algorithm with adaptive feeding," *Electronics Letters*, Vol. 39, No. 15, July 24, 2003.

8. Moses, R., L. Potter, H. Chiang, M. Koets, and A. Sabharwal, "A parametric attributed scattering center model for SAR automatic target recognition," *1998 Image Understanding Workshop*, Pacific Grove, CA, Nov. 20–23, 1998.

9. Wang, Y. and H. Ling, "Efficient radar signature prediction using a frequency-aspect interpolation technique based on adaptive feature extraction," *IEEE Transactions on Antennas and Propagation*, Vol. 50, No. 2, 122–131, Feb. 2002.

10. Hogbörn, J. A., "Aperture synthesis with a nonregular distribution of interferometric baselines," *Astronomy and Astrophysics Supplements*, Vol. 15, 417–426, 1974.

11. Mallat, S. G. and Z. Zhang, "Matching pursuits with time-frequency dictionaries," *IEEE Transactions on Signal Processing*, Vol. 41, 3397–3415, Dec. 1993.

12. Li, J. and P. Stoica, "Efficient mixed-spectrum estimation with applications to target feature extraction," *IEEE Transactions on Signal Processing*, Vol. 44, No. 2, Feb. 1996.